Mechanistic Investigation of Photon Upconversion in Nd³⁺-Sensitized Core−Shell Nanoparticles

Xiaoji Xie,[†] Nengyue Gao,[†] Renren Deng,[†] Qiang Sun,[†] Qing-Hua Xu,[†] and Xiaogang Liu*[,†,‡]

[†]Department of Chemistry, National University of Singapore, 3 Science Drive 3, Singapore 117543, Singapore
[‡]Institute of Materials Research and Engineering, 3 Research Link, Singapore 117602, Singapore

Ⓢ *Supporting Information*

ABSTRACT: A new type of core−shell upconversion nanoparticles which can be effectively excited at 795 nm has been designed and synthesized through spatially confined doping of neodymium (Nd³⁺) ions. The use of Nd³⁺ ions as sensitizers facilitates the energy transfer and photon upconversion of a series of lanthanide activators (Er³⁺, Tm³⁺, and Ho³⁺) at a biocompatible excitation wavelength (795 nm) and also significantly minimizes the overheating problem associated with conventional 980 nm excitation. Importantly, the core−shell design enabled high-concentration doping of Nd³⁺ (∼20 mol %) in the shell layer and thus markedly enhanced the upconversion emission from the activators, providing highly attractive luminescent biomarkers for bioimaging without autofluorescence and concern of overheating.

Lanthanide-doped luminescent upconversion nanoparticles of various compositions have been widely investigated over the past few years.[1] These upconversion nanoparticles have shown potential applications in diverse fields.[2] In particular, their unique optical properties, including narrow emission bandwidths, large anti-Stokes shifts, long luminescence lifetimes, and high photostability, make them more suitable as biomarkers than conventionally used organic dyes or quantum dots.[2] Despite these advances, there exist a number of daunting challenges that may prevent widespread use of upconversion nanoparticles in practical biological settings.[3] One notable challenge is the requirement of an excitation wavelength near 980 nm, which matches the absorption by Yb³⁺ ions commonly doped into nanoparticles as sensitizers. Unfortunately, the absorption of Yb³⁺ ions largely overlaps the absorption band of water molecules that are dominant in biological samples (Figure S1 in the Supporting Information).[4,5] Therefore, the 980 nm excitation source would be significantly attenuated while passing through biological samples. Moreover, overexposure of biological species under 980 nm irradiation would cause overheating issues, resulting in significant cell death and tissue damage.

Recently, considerable efforts have been devoted to finding suitable excitation wavelengths within the "biological window".[5] In principle, the overheating effect induced by 980 nm excitation could be largely alleviated using 800 nm laser excitation because of low absorption coefficients displayed by water molecules and biological tissues at 800 nm. Photon upconversion under 800 nm excitation can be achieved through use of Nd³⁺ ions as the sensitizer, as Nd³⁺ features a sharp absorption band centered around 800 nm.[5,6] However, this design allows only for doping of Nd³⁺ at very low concentrations (typically <2%) in either bulk or nanoparticle systems, leading to weak absorption at 800 nm and thus weak upconverted emission.[5e,6] An elevated amount of Nd³⁺ ions, especially those doped in nanoscale systems, can largely induce deleterious cross-relaxation between the Nd³⁺ ions and the activator ions. This cross-relaxation would consume most of the excitation energy. Therefore, even with passivation using an inert shell of NaYF₄, the upconversion emission of Nd³⁺-based nanoparticles upon 800 nm irradiation is weak relative to that of Yb³⁺-based counterparts involving 980 nm excitation.[5e] A core−shell strategy involving the doping of Yb³⁺ and Nd³⁺ in the shell layer may enhance energy transfer from Nd³⁺ to Yb³⁺,[5f] but luminescence quenching of surface Yb³⁺ dopants in the shell layer becomes a signficant constraint.

Herein we introduce a rational core−shell strategy that provides precise control over the concentration of dopant ions in the core and shell layers of nanoparticles (Figure 1). In our design, a small amount of Nd³⁺ ions (1−2 mol %) is doped into the core particle to minimize concentration quenching, while a relatively high concentration of Nd³⁺ ions (∼20 mol %) is selectively doped within the shell layer for effective harvesting of light with wavelengths around 800 nm.[7] Notably, the absorption intensity at 794 nm for the nanoparticles with 20 mol % Nd³⁺ in the shell layer was ∼17 times higher than that for the controls without Nd³⁺ in the shell layer (Figure 1b). It should be noted that we avoid codoping of Yb³⁺ with Nd³⁺ in the shell layer to minimize surface quenching.[5f] Remarkably, we found that the absorption intensity recorded at 794 nm for Nd³⁺ (20 mol % in the shell layer) was almost 5 times stronger than that at 976 nm for Yb³⁺ (30 mol % in the core layer) (Figure 1b). This result implies the feasibility of using Nd³⁺-sensitized core−shell nanoparticles that may render upconversion performance comparable to that of conventionally used Yb³⁺-based nanoparticles.

As a proof-of-concept experiment, we chose NaYF₄ as the host material because of its documented high upconversion efficiency.[8] In a typical experiment, we first synthesized NaYF₄ core nanoparticles triply doped with Yb³⁺, Nd³⁺, and A³⁺ (A = Tm, Er, Ho) according to a previously reported method.[9] Transmission electron microscopy (TEM) images of the as-synthesized nanoparticles (Figure 2a−c) indicated a single-crystalline hexagonal structure of the nanoparticles. We then studied the upconversion profile of the NaYF₄:Yb/Tm/Nd
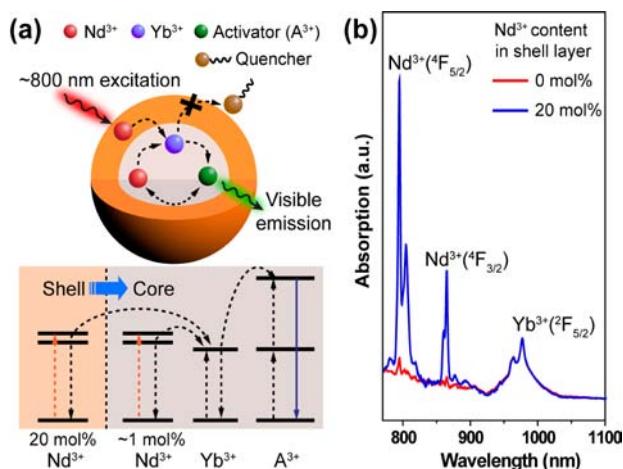
Figure 1. (a) Schematic design (top) and simplified energy level diagram (bottom) of a core−shell nanoparticle for photon upconversion under 800 nm excitation. Nd^{3+} ions doped in the core and shell layers serve as sensitizers to absorb the excitation energy and subsequently transfer it to Yb^{3+} ions. After energy migration from the Yb^{3+} ions to activator ions, activator emission is achieved via the Nd^{3+}-sensitization process. (b) Near-IR absorption spectra of $NaYF_4$:Yb/Nd(30/1%) nanoparticles coated with an inert $NaYF_4$ shell or an active $NaYF_4$:Nd(20%) shell. The absorption spectra were normalized at 976 nm for comparison.

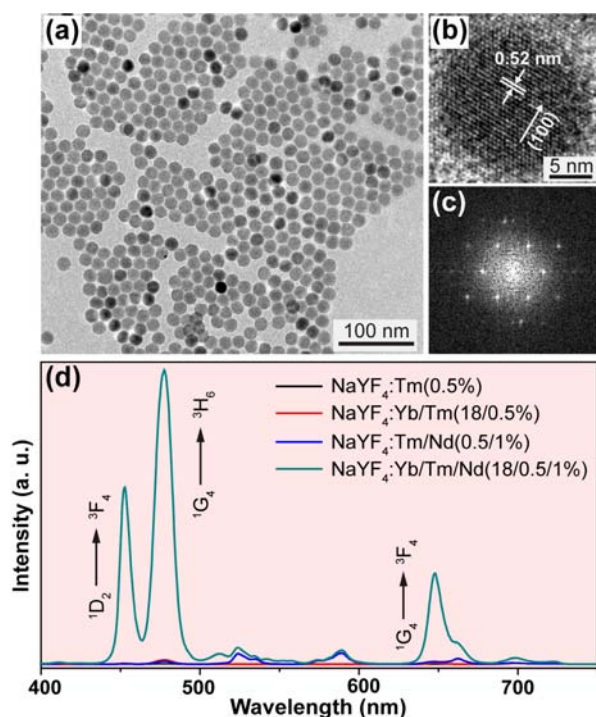**Figure 2.** (a) Low-resolution TEM image of the as-synthesized $NaYF_4$:Yb/Tm/Nd(18/0.5/1%) nanoparticles. (b) High-magnification TEM image showing the single-crystalline structure of a nanoparticle. (c) Fourier transform diffraction pattern of the TEM image in (b). (d) Room-temperature upconversion emission spectra of $NaYF_4$ nanoparticles with different dopants (~1 wt % in cyclohexane). The spectra were recorded under excitation by a 795 nm continuous-wave (CW) laser at a power of 50 mW.

nanoparticles using a 795 nm laser. As anticipated, the triply doped nanoparticles could be excited under 795 nm irradiation, giving rise to characteristic emission peaks of Tm^{3+} (Figure 2d).

In sharp contrast, we were unable to generate noticeable Tm^{3+} emission from nanoparticles with no Nd^{3+} added (Figure 2d). Our control experiment showed that the Yb^{3+} ion also plays an important role in facilitating energy transfer from Nd^{3+} to the activator ions.

We next carried out experiments to optimize the doping concentration in triply doped $NaYF_4$ nanoparticles (Figures S6−S8). We found that the optimum Nd^{3+} concentration for efficient upconversion under 800 nm excitation was 1−2%, which is in good agreement with that reported by the Han group.[5e] Although higher Nd^{3+} concentrations would favor sensitization, the high doping level could inevitably lead to localized concentration quenching of activator emissions caused by enhanced cross-relaxation between the lanthanide ions. It should be mentioned that the emission color of the Nd^{3+}-sensitized $NaYF_4$ nanoparticles could also be tuned by varying the doping concentrations in a fashion similar to that for Yb^{3+}-sensitized nanoparticles.[10]

To enhance the sensitization to 800 nm irradiation with minimized deleterious cross-relaxation, we prepared a series of triply doped core−shell nanoparticles with active Nd^{3+} shell coatings (Figure S11). With the assistance of this active-shell design, we were able to dope an elevated amount of Nd^{3+} ions into the nanoparticles and achieve improved emissions from Tm^{3+}, Er^{3+}, and Ho^{3+} activators (Figure 3). For example, the $NaYF_4$:Yb/Tm/Nd@$NaYF_4$:Nd core−shell nanoparticles with 20 mol % Nd^{3+} in the shell layer showed an integrated emission intensity ~405 times higher than that achievable using the nanoparticles without the shell coating (Figure 3a). Importantly, the active-shell coating strategy achieved an emission intensity ~7 times higher than the one obtained with an inert $NaYF_4$ shell. The activator emissions of the Nd^{3+}-sensitized core−shell nanoparticles could easily be visualized by the naked eye (Figure 3).

In an attempt to understand the mechanisms underlying the Nd^{3+}-sensitized upconversion process (Figure S14), we further conducted a set of control experiments. For nanoparticles codoped with Nd^{3+} (1 mol %) and activator ions, the activator ion receives the energy from a nearby Nd^{3+} sensitizer ion. This was confirmed by the fact that the Nd^{3+} $^4F_{3/2}$ lifetime decreased when the Nd^{3+} ion was situated at random in a nanoparticle around an activator ion (Figure S15). However, the energy transfer from Nd^{3+} to the activator was inefficient because of the low doping concentration. By comparison, a nearly 90% efficiency was observed for energy transfer between the Nd^{3+} $^4F_{3/2}$ and Yb^{3+} $^2F_{5/2}$ states (Figure 4a). The efficient transfer of excitation energy from Nd^{3+} to Yb^{3+} was further supported by the observation of Yb^{3+} emission at 976 nm (Figure S16). These results suggest that the Yb^{3+} ions can act as efficient energy migrators, facilitating energy transfer from Nd^{3+} ions to activator ions.

To validate the effect of the core−shell structure on the enhancement of activator emission, we prepared a series of nanoparticles doped without activators. A significant increase in the Yb^{3+} $^2F_{5/2}$ lifetime was observed when either an inert $NaYF_4$ shell or an active $NaYF_4$:Nd shell was applied to $NaYF_4$:Nd/Yb nanoparticles (Figure 4b). The Yb^{3+} $^2F_{5/2}$ lifetimes recorded for nanoparticles having the active $NaYF_4$:Nd shell and the inert $NaYF_4$ shell were essentially identical. However, the active-shell-modified nanoparticles exhibited much stronger Yb^{3+} emission than their inert-shell-modified counterparts (Figure 4c). Taken together, these data suggest that the active $NaYF_4$:Nd shell layer can effectively prevent surface quenching of Yb^{3+} emission and
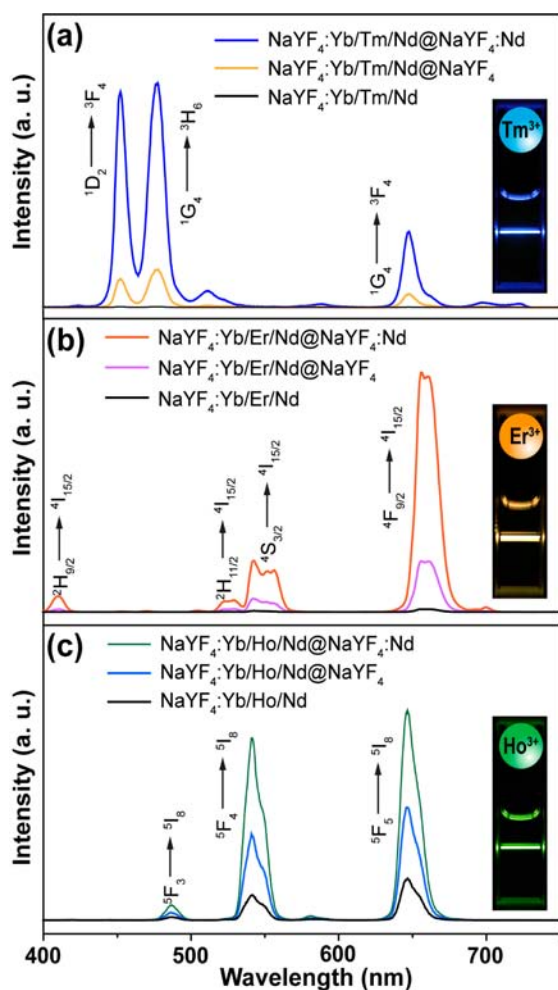
Figure 3. Photoluminescence investigations of Nd^{3+}-sensitized upconversion in a series of lanthanide-doped upconversion nanoparticles dispersed in cyclohexane. (a) Upconversion emission spectra for NaYF$_4$:Yb/Tm/Nd(30/0.5/1%) nanoparticles and the corresponding core−shell nanoparticles coated with an inert NaYF$_4$ shell or an active NaYF$_4$:Nd(20%) shell. (b) Upconversion emission spectra for NaYF$_4$:Yb/Er/Nd(30/0.5/1%) nanoparticles and the corresponding core−shell nanoparticles coated with NaYF$_4$ or NaYF$_4$:Nd(20%). (c) Upconversion emission spectra for NaYF$_4$:Yb/Ho/Nd(10/1/2%) nanoparticles and the corresponding core−shell nanoparticles coated with NaYF$_4$ or NaYF$_4$:Nd(20%). The insets are the corresponding luminescence photographs of solutions containing active-shell-coated nanoparticles. All of the spectra were recorded under excitation by a 795 nm CW laser at a power of 20 mW. For intensity comparison, the absorption spectra were normalized at 976 nm.

simultaneously can promote the transfer of excitation energy to Yb^{3+} ions. It should be noted that the emission of Nd^{3+} ions doped on the surface of the nanoparticles was not significantly affected by surface quenching, as evidenced by the slight change in the Nd^{3+} $^4F_{3/2}$ lifetime after the NaYF$_4$:Nd nanoparticle was coated with an inert NaYF$_4$ shell (Figure S17).

To confirm the upconversion emission promoted by the active shell upon excitation at 795 nm, we benchmarked the emission intensity of nanoparticles obtained upon 795 nm excitation using the active NaYF$_4$:Nd shell design with those of commonly used Yb^{3+}-sensitized core−shell nanoparticles requiring 980 nm excitation (Figure 4d,e). Inspiringly, the Nd^{3+}-sensitized nanoparticles rendered upconversion performance comparable to that of the Yb^{3+}-based nanoparticles.
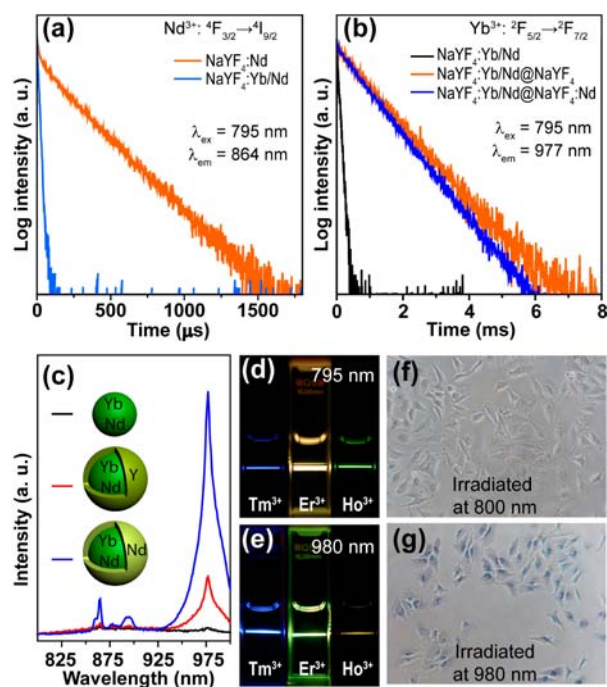

Figure 4. (a) Nd^{3+} decay curves recorded for NaYF$_4$:Nd(1%) nanoparticles with and without Yb^{3+}(30%) codoping. (b) Yb^{3+} decay curves recorded for NaYF$_4$:Yb/Nd(30/1%) nanoparticles and the corresponding core−shell nanoparticles coated with NaYF$_4$ or NaYF$_4$:Nd(20%). (c) Near-IR photoluminescence spectra of the nanoparticles shown in (b). (d, e) Luminescence photographs of activator emissions (Tm 0.5%, Er 0.5%, Ho 1%) for Nd^{3+}-sensitized and Yb^{3+}-sensitized nanoparticles under 795 and 980 nm irradiation, respectively (laser power: 100 mW). The same particle concentration for each set of comparisons was obtained by normalizing the particle absorption at 976 nm. (f, g) Optical microscopy images of trypan blue-treated HeLa cells recorded after irradiation for 5 min at 800 and 980 nm, respectively (6 W/cm^2).

The use of Nd^{3+} ions as the sensitizers for 800 nm excitation is likely to significantly minimize the heating effect typically associated with Yb^{3+} sensitization for the corresponding 980 nm excitation. To highlight the benefits of using 800 nm excitation, we compared cell viabilities of HeLa cells irradiated at 800 and 980 nm, respectively (Figure S19). The trypan blue test showed that almost all of the cancer cells were killed when irradiated for 5 min with the 980 nm laser (Figure 4g). By comparison, the cancer cells remained intact after 800 nm illumination under identical conditions (Figure 4f).

In conclusion, we have developed a new class of upconversion nanoparticles based on the combination of Nd^{3+} sensitization and an active-shell design that exhibit efficient activator emission upon excitation near 800 nm. This study, although quite preliminary in many respects, represents an important advance in the development of luminescent markers suitable for biolabeling applications. On a broader level, the wide spectrum of different activator types coupled with versatile core−shell approaches greatly expands the horizons of existing upconversion nanomaterials, enabling in situ imaging of biological and chemical events without overheating issues. We anticipate that these nanoparticles will help stimulate new areas of investigation and illuminate many aspects of research relevant to human health and disease.

ASSOCIATED CONTENT

S Supporting Information

Additional experimental details. This material is available free of charge via the Internet at http://pubs.acs.org.

AUTHOR INFORMATION

Corresponding Author

chmlx@nus.edu.sg

Notes

The authors declare no competing financial interest.

ACKNOWLEDGMENTS

REFERENCES

(1) (a) Haase, M.; Schäfer, H. *Angew. Chem., Int. Ed.* **2011**, *50*, 5808. (b) Liu, Y.; Zhou, S.; Tu, D.; Chen, Z.; Huang, M.; Zhu, H.; Ma, E.; Chen, X. *J. Am. Chem. Soc.* **2012**, *134*, 15083. (c) Xue, X.; Wang, F.; Liu, X. *J. Mater. Chem.* **2011**, *21*, 13107. (d) Zhou, J.; Liu, Z.; Li, F. *Chem. Soc. Rev.* **2012**, *41*, 1323. (e) Wang, F.; Banerjee, D.; Liu, Y.; Chen, X.; Liu, X. *Analyst* **2010**, *135*, 1839. (f) Feng, W.; Sun, L.; Zhang, Y.; Yan, C. *Coord. Chem. Rev.* **2010**, *254*, 1038. (g) Li, C.; Lin, J. *J. Mater. Chem.* **2010**, *20*, 6831. (h) Liu, Y.; Tu, D.; Zhu, H.; Ma, E.; Chen, X. *Nanoscale* **2013**, *5*, 1369. (i) Su, L.; Karuturi, S. K.; Luo, J.; Liu, L.; Liu, X.; Guo, J.; Sum, T. C.; Deng, R.; Fan, H.; Liu, X.; Tok, A. Y. *Adv. Mater.* **2013**, *25*, 1603. (j) Wang, C.; Chen, L.; Liu, Y.; Wang, X.; Ma, X.; Deng, Z.; Li, Y.; Liu, Z. *Adv. Funct. Mater.* **2013**, *23*, 3077. (k) Xu, C. T.; Svenmarker, P.; Liu, H.; Wu, X.; Messing, M. E.; Wallenberg, R.; Andersson-Engels, S. *ACS Nano* **2012**, *6*, 4788. (l) Gorris, H. H.; Wolfbeis, O. S. *Angew. Chem., Int. Ed.* **2013**, *52*, 3584. (m) Wu, W.; Yao, L.; Yang, T.; Yin, R.; Li, F.; Yu, Y. *J. Am. Chem. Soc.* **2011**, *133*, 15810.

(2) (a) Wang, M.; Mi, C.; Wang, W.; Liu, C.; Wu, Y.; Xu, Z.; Mao, C.; Xu, S. *ACS Nano* **2009**, *3*, 1580. (b) Yang, Y.; Shao, Q.; Deng, R.; Wang, C.; Teng, X.; Cheng, K.; Cheng, Z.; Huang, L.; Liu, Z.; Liu, X.; Xing, B. *Angew. Chem., Int. Ed.* **2012**, *51*, 3125. (c) Zhang, F.; Shi, Q.; Zhang, Y.; Shi, Y.; Ding, K.; Zhao, D.; Stucky, G. D. *Adv. Mater.* **2011**, *23*, 3775. (d) Deng, R.; Xie, X.; Vendrell, M.; Chang, Y.-T.; Liu, X. *J. Am. Chem. Soc.* **2011**, *133*, 20168. (e) Mai, H.; Zhang, Y.; Si, R.; Yan, Z.; Sun, L.; You, L.; Yan, C. *J. Am. Chem. Soc.* **2006**, *128*, 6426. (f) Teng, X.; Zhu, Y.; Wei, W.; Wang, S.; Huang, J.; Naccache, R.; Hu, W.; Tok, A. I. Y.; Han, Y.; Zhang, Q.; Fan, Q.; Huang, W.; Capobianco, J. A.; Huang, L. *J. Am. Chem. Soc.* **2012**, *134*, 8340. (g) Liu, Y.; Chen, M.; Cao, T.; Sun, Y.; Li, C.; Liu, Q.; Yang, T.; Yao, L.; Feng, W.; Li, F. *J. Am. Chem. Soc.* **2013**, *135*, 9869. (h) Tian, G.; Ren, W.; Yan, L.; Jian, S.; Gu, Z.; Zhou, L.; Jin, S.; Yin, W.; Li, S.; Zhao, Y. *Small* **2013**, *9*, 1929. (i) Jin, J.; Gu, Y.; Man, C. W.; Cheng, J.; Xu, Z.; Zhang, Y.; Wang, H.; Lee, V. H.; Cheng, S. H.; Wong, W. T. *ACS Nano* **2011**, *5*, 7838. (j) Park, Y. I.; Kim, H. M.; Kim, J. H.; Moon, K. C.; Yoo, B.; Lee, K. T.; Lee, N.; Choi, Y.; Park, W.; Ling, D.; Na, K.; Moon, W. K.; Choi, S. H.; Park, H. S.; Yoon, S.; Suh, Y. D.; Lee, S. H.; Hyeon, T. *Adv. Mater.* **2012**, *24*, 5755. (k) Idris, N. M.; Gnanasammandhan, M. K.; Zhang, J.; Ho, P. C.; Mahendran, R.; Zhang, Y. *Nat. Med.* **2012**, *18*, 1580. (l) Li, L.; Zhang, R.; Yi, L.; Zheng, K.; Qin, W.; Selvin, P.; Lu, Y. *Angew. Chem., Int. Ed.* **2012**, *51*, 6121.

(3) (a) Wang, F.; Deng, R.; Wang, J.; Wang, Q.; Han, Y.; Zhu, H.; Chen, X.; Liu, X. *Nat. Mater.* **2011**, *10*, 968. (b) Hao, J.; Zhang, Y.; Wei, X. *Angew. Chem., Int. Ed.* **2011**, *50*, 6876. (c) Li, L.; Wu, P.; Hwang, K.; Lu, Y. *J. Am. Chem. Soc.* **2013**, *135*, 2411. (d) Johnson, N. J. J.; Korinek, A.; Dong, C.; van Veggel, F. C. J. M. *J. Am. Chem. Soc.* **2012**, *134*, 11068. (e) Park, Y. I.; Nam, S. H.; Kim, J. H.; Bae, Y. M.; Yoo, B.; Kim, H. M.; Jeon, K.; Park, H. S.; Choi, J. S.; Lee, K. T.; Suh, Y. D.; Hyeon, T. *J. Phys. Chem. C* **2013**, *117*, 2239. (f) Bogdan, N.; Vetrone, F.; Ozin, G. A.; Capobianco, J. A. *Nano Lett.* **2011**, *11*, 835. (g) Chen, G.; Ohulchanskyy, T. Y.; Liu, S.; Law, W.; Wu, F.; Swihart, M. T.; Agren, H.; Prasad, P. N. *ACS Nano* **2012**, *6*, 2969. (h) Wang, Y.; Tu, L.; Zhao, J.; Sun, Y.; Kong, X.; Zhang, H. *J. Phys. Chem. C* **2009**, *113*, 7164. (i) Ye, X.; Chen, J.; Engel, M.; Millan, J. A.; Li, W.; Qi, L.; Xing, G.; Collins, J. E.; Kagan, C. R.; Li, J.; Glotzer, S. C.; Murray, C. B. *Nat. Chem.* **2013**, *5*, 466.

(4) (a) Weissleder, R. *Nat. Biotechnol.* **2001**, *19*, 316. (b) Byrnes, K. R.; Waynant, R. W.; Ilev, I. K.; Wu, X.; Barna, L.; Smith, K.; Heckert, R.; Gerst, H.; Anders, J. J. *Lasers Surg. Med.* **2005**, *36*, 171.

(5) (a) Zhan, Q.; Qian, J.; Liang, H.; Somesfalean, G.; Wang, D.; He, S.; Zhang, Z.; Andersson-Engels, S. *ACS Nano* **2011**, *5*, 3744. (b) Zhan, Q.; He, S.; Qian, J.; Cheng, H.; Cai, F. *Theranostics* **2013**, *3*, 306. (c) Zou, W.; Visser, C.; Maduro, J. A.; Pshenichnikov, M. S.; Hummelen, J. C. *Nat. Photonics* **2012**, *6*, 560. (d) Xie, X.; Liu, X. *Nat. Mater.* **2012**, *11*, 842. (e) Shen, J.; Chen, G.; Vu, A.-M.; Fan, W.; Bilsel, O. S.; Chang, C.-C.; Han, G. *Adv. Opt. Mater.* **2013**, DOI: 10.1002/adom.201300160. (f) Wang, Y.-F.; Liu, G.-Y.; Sun, L.-D.; Xiao, J.-W.; Zhou, J.-C.; Yan, C.-H. *ACS Nano* **2013**, DOI: 10.1021/nn402601d.

(6) (a) Librantz, A. F. H.; Gomes, L.; Courrol, L. C.; Ranieri, I. M.; Baldochi, S. L. *J. Appl. Phys.* **2009**, *105*, No. 113503. (b) Lin, H.; Chen, D.; Yu, Y.; Shan, Z.; Huang, P.; Wang, Y.; Yuan, J. *J. Appl. Phys.* **2010**, *107*, No. 103511. (c) Balda, R.; Pena, J. I.; Arriandiaga, M. A.; Fernandez, J. *Opt. Express* **2010**, *18*, 13842. (d) Zhou, J.; Shirahata, N.; Sun, H.-T.; Ghosh, B.; Ogawara, M.; Teng, Y.; Zhou, S.; Chu, R. G. S.; Fujii, M.; Qiu, J. *J. Phys. Chem. Lett.* **2013**, *4*, 402. (e) Liu, Y.; Wang, D.; Shi, J.; Peng, Q.; Li, Y. *Angew. Chem., Int. Ed.* **2013**, *52*, 4366.

(7) (a) Vetrone, F.; Naccache, R.; Mahalingam, V.; Morgan, C. G.; Capobianco, J. A. *Adv. Funct. Mater.* **2009**, *19*, 2924. (b) Yang, D.; Li, C.; Li, G.; Shang, M.; Kang, X.; Lin, J. *J. Mater. Chem.* **2011**, *21*, 5923.

(8) (a) Wang, F.; Han, Y.; Lim, C. S.; Lu, Y.; Wang, J.; Xu, J.; Chen, H.; Zhang, C.; Hong, M.; Liu, X. *Nature* **2010**, *463*, 1061. (b) Yin, M.; Wu, L.; Li, Z.; Ren, J.; Qu, X. *Nanoscale* **2012**, *4*, 400. (c) Zhao, J.; Lu, Z.; Yin, Y.; McRae, C.; Piper, J. A.; Dawes, J. M.; Jin, D.; Goldys, E. M. *Nanoscale* **2013**, *5*, 944. (d) Schäfer, H.; Ptacek, P.; Eickmeier, H.; Haase, M. *Adv. Funct. Mater.* **2009**, *19*, 3091. (e) Ye, X.; Collins, J. E.; Kang, Y.; Chen, J.; Chen, D. T. N.; Yodh, A. G.; Murray, C. B. *Proc. Natl. Acad. Sci. U.S.A.* **2010**, *107*, 22430.

(9) (a) Su, Q.; Han, S.; Xie, X.; Zhu, H.; Chen, H.; Chen, C. K.; Liu, R. S.; Chen, X.; Wang, F.; Liu, X. *J. Am. Chem. Soc.* **2012**, *134*, 20849. (b) Wang, F.; Wang, J.; Liu, X. *Angew. Chem., Int. Ed.* **2010**, *49*, 7456.

(10) (a) Wang, F.; Liu, X. *J. Am. Chem. Soc.* **2008**, *130*, 5642. (b) Wang, J.; Wang, F.; Xu, J.; Wang, Y.; Liu, Y.; Chen, X.; Chen, H.; Liu, X. *C. R. Chim.* **2010**, *13*, 731. (c) Chen, D.; Yu, Y.; Huang, F.; Yang, A.; Wang, Y. *J. Mater. Chem.* **2011**, *21*, 6186. (d) Chen, G.; Qiu, H.; Fan, R.; Hao, S.; Tan, S.; Yang, C.; Han, G. *J. Mater. Chem.* **2012**, *22*, 20190. (e) Wang, J.; Wang, F.; Wang, C.; Liu, Z.; Liu, X. *Angew. Chem., Int. Ed.* **2011**, *50*, 10369.